# Spectral anomalies of waveguide electromagnetic modes in layered structures

© V.I. Alshits, M. Deschamps*, E. Ducasse*, V.N. Lyubimov, G.A. Maugin**

A.V. Shubnikov Institute of Crystallography, Russian Academy of Sciences,
119333 Moscow, Russia
* Laboratoire de Mécanique Physique, Université Bordeaux 1, CNRS, UMR 5469,
33405 Talence, France
** Laboratoire de Modélisation en Mécanique, Université Pierre et Marie Curie / CNRS, UMR 7607,
75252 Paris, France

E-mail: alshits@ns.crys.ras.ru

(Received July 16, 2007)

A theoretical study of electromagnetic guided eigenwaves in two- and three-layered plates with metallized surfaces is accomplished. The appropriate dispersion equations are explicitly analyzed on the basis of some deiscretization, first introduced in Mindlin's theory of Lamb acoustic waves. It is shown that the dispersion branches of independent eigenmode families cross each other in the nodes of some grid formed by two infinite series of bond lines. The latter represent the dispersion curves for homogeneous plates with permittivities $\varepsilon_1$ or $\varepsilon_2$ coinciding with those for the layers of the wavegiude. It is proved that, beyond nodes of the grid, the dispersion curves may not intersect bond lines, which thus provide definite „corridors" for these curves. The dispersion lines have a wavy („zigzag") form in the grid zone and remain smooth beyond the grid. The crossing branches have coinciding cutoff frequencies. In the dimensionless coordinates „slowness $(S)$ vs frequency $(f)$" the branches $S_l(f)$ have two asymptotic levels: $S = \sqrt{\varepsilon_1}$ and $S = \sqrt{\varepsilon_2}$. At the lower one, the spectrum forms a step-like terracing pattern with a progressive closing to the asymptote of a succession of dispersion curves, which change each other at this level with further going up to the next asymptote. An extension to anisotropic waveguides with layers made of uniaxial crystals is considered.

PACS: 41.20.Jb, 42.25.Gy

## 1. Introduction

Due to its very important practical applications, the physics of optical waveguides is a rather popular field, which has a long history of extensive investigations (see, e.g., [1–5]). Of course it is not a closed field. There are many different aspects in this domain of science some of which still are waiting for their study. The most theoretical results in this field are obtained by numerical methods. So the development and improvement of these methods represent a big part of activity here. On the other hand, in many cases a more effective approach is provided by a combination of analytical and computational analyses, especially when one deals with properties and phenomena which have unusual and anomalous features. We have a definite experience in studying such specific effects in waveguides, both optical and acoustical [6–12].

This paper was especially stimulated by the last mentioned paper [12] in the above recalled series where some peculiarities were found in spectra of SH guided acoustic waves in two- and three-layered elastic plates. In particular, it turned out that dispersion curves manifest a wavy („zigzag") form in some spectral zone and intersect each other in the nodes of a definite grid, which can be analytically described. This turns out to be very similar to the grid introduced by Mindlin [13] in his theory of acoustic Lamb waves in a homogeneous elastic plate (see also the papers [14–16]). The other important feature of the spectrum of SH acoustic waves was an unusual asymptotic behavior of despersion branches at an intermediate level where they form a step-like terracing pattern changing each other in the vicinity of this level with a successive closing to the level and further going to the next asymptote. Analogous patterns were earlier described in [10] as anisotropic effects in acoustic spectra for a homogeneous plate.

Here below, analogous peculiarities will be found in spectra of electromagnetic modes in similar two- and three-layered waveguides composed of isotropic materials with a metallization at the surfaces. We in fact present a complete analysis of the problem by combining analytical and numerical methods. The structure of all wave fields is derived and the corresponding dispersion equations are analyzed. Mindlin's idea of a specific „discretization" of the problem proves again to be applicable. In particular, we find thus the intersection points of dispersion lines of independent families for the two types of waveguides and some other characteristic points of the studied spectra. It is shown that, unlike in acoustics, the crossing pairs of independent dispersion lines are characterized by coinciding cutoff frequencies. And, again in contrast to acoustics, it is proved that the branch crossing beyound Mindlin's grid is forbidden. The extension of the theory to the case of anisotropic layers made of uniaxial crystals with fundamental axes orthogonal to the sagittal plane is finally considered. In the end, we also compare the found electromagnetic spectral features with the acoustic properties in similar waveguide structures.

## 2. Basic equations and conditions at surfaces and interfaces

In this paper, we consider electromagnetic eigenmodes in two- and three-layered plates with metallized surfaces (Fig. 1). The layers are formed by two isotropic dielectric materials with permittivities $\varepsilon_1$ and $\varepsilon_2$ supposed to be dimensionless parameters being expressed in the CGSE system. In such media, bulk electromagnetic waves propagate with the phase speeds

$$c_1 = c/N_1, \quad c_2 = c/N_2, \tag{1}$$

where $c$ is the speed of light in vacuum and $N_j = \sqrt{\varepsilon_j}$ is the refractive index of the layer $j$. In further considerations we shall suppose that $\varepsilon_1 < \varepsilon_2$, then accordingly $N_1 < N_2$ and $c_1 > c_2$.

As usual [3–5], the studied waveguide modes in each of the layers must have a structure of a combination of two partial waves with wave vectors belonging to the sagittal plane $(xy)$ and differing only by the sign of their $y$-components: $\mathbf{k}_j^{\pm} = k(1, \pm p_j, 0)$. For instance, the structure of the electromagnetic wave field in a two-layered plate is described by

$$\begin{bmatrix} \mathbf{E}(x,y;t) \\ \mathbf{H}(x,y;t) \end{bmatrix} = \begin{bmatrix} \mathbf{E}(y) \\ \mathbf{H}(y) \end{bmatrix} \exp[ik(x - vt)], \tag{2}$$

$$\begin{bmatrix} \mathbf{E}(y) \\ \mathbf{H}(y) \end{bmatrix} = \begin{cases} A_1^+ \begin{bmatrix} \mathbf{E}_1^+ \\ \mathbf{H}_1^+ \end{bmatrix} \exp(ikp_1 y) \\ \quad + A_1^- \begin{bmatrix} \mathbf{E}_1^- \\ \mathbf{H}_1^- \end{bmatrix} \exp(-ikp_1 y), \ 0 \le y \le d_1; \\ A_2^+ \begin{bmatrix} \mathbf{E}_2^+ \\ \mathbf{H}_2^+ \end{bmatrix} \exp(ikp_2 y) \\ \quad + A_2^- \begin{bmatrix} \mathbf{E}_2^- \\ \mathbf{H}_2^- \end{bmatrix} \exp(-ikp_2 y), \ -d_2 \le y \le 0. \end{cases} \tag{3}$$

In Eq. (2), $v = \omega/k$ is the tracing speed and $\omega$ is the frequency of the electromagnetic wave.

The parameters $p_j$ and the vectors $\mathbf{E}_j^{\pm}, \mathbf{H}_j^{\pm}$ in (3) must be chosen so that each of partial waves would satisfy Maxwell's equations [17,18]. The sagittal plane $xy$ of wave propagation in Fig. 1 is a symmetry plane, therefore polarizations $\mathbf{E}_j^{\pm}, \mathbf{H}_j^{\pm}$ may be either orthogonal or parallel to this plane. In accordance with Maxwell's equations, these components are not independent and in one wave the transversely polarized electric field must be accompanied by the in-plane polarized magnetic field and *vice versa*. We shall denote these combinations as $TE$ and $TM$ modes, respectively: in the first one $\mathbf{E} \parallel z$, $\mathbf{H} \perp z$, in the second $\mathbf{H} \parallel z$, $\mathbf{E} \perp z$. The result valid for any boundary conditions

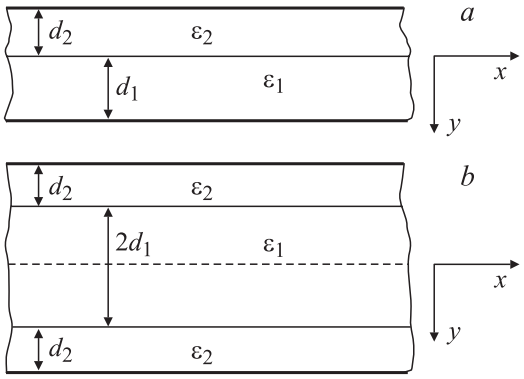


**Figure 1.** Considered sandwich structures: two-layered ($a$) and symmetric three-layered ($b$) plates. Thicklined boundaries indicate metallized surfaces. Homogeneous fragments of the two structures are formed by isotropic media with electric permittivities $\varepsilon_1$ and $\varepsilon_2$.

is known [3,9] and in our terms looks as

$$\begin{bmatrix} \mathbf{E}_j^{\pm} \\ \mathbf{H}_j^{\pm} \end{bmatrix}^{TE} = \begin{bmatrix} (0,0,1) \\ (c/v)(\pm p_j, -1, 0) \end{bmatrix},$$

$$\begin{bmatrix} \mathbf{E}_j^{\pm} \\ \mathbf{H}_j^{\pm} \end{bmatrix}^{TM} = \begin{bmatrix} (c/v)(\mp p_j, 1, 0)/\varepsilon_j \\ (0,0,1) \end{bmatrix}, \tag{4}$$

$$p_j \equiv p_j(v) = \sqrt{(v/c_j)^2 - 1}, \quad j = 1, 2. \tag{5}$$

On the other hand, the amplitudes $A_j^{\pm}$ in (3) and the dispersion spectrum $v = v_n(k)$ are completely determined by conditions at surfaces and interfaces. At the interfaces the tangential projections of the two fields $\mathbf{E}$ and $\mathbf{H}$ must be continuous:

$$\mathbf{E}_t(y_{\text{interf}} + 0) = \mathbf{E}_t(y_{\text{interf}} - 0),$$
$$\mathbf{H}_t(y_{\text{interf}} + 0) = \mathbf{H}_t(y_{\text{interf}} - 0). \tag{6}$$

The surfaces of our waveguide sandwich structures (Fig. 1) are supposed to be coated by metal films. At such boundaries for not very high frequency $\omega$ the tangential electric field components $\mathbf{E}_t$ must vanish [17],

$$\mathbf{E}_t\big|_{\text{surf}} = 0. \tag{7}$$

Strictly speaking, condition (7) is fulfilled only on a boundary with a perfect conductor which has a zero surface impedance $\xi$. For real metals at not small frequencies $\omega$, the impedance $\xi$ does not vanish and, instead of (7), one should rather use the boundary condition [17] $\mathbf{E}_t = \xi[\mathbf{H}_t\mathbf{n}]$, where $\mathbf{n}$ is the inside normal to the surface. However, for good conductors there are wide frequency ranges where $|\xi| \ll 1$ and condition (7) is applicable. This occurs for infrared optical wavelengths in many metals and sometimes holds up to a middle of visible range (e.g., for pure Al at 295 K [19]: $|\xi| \approx 1/40$; 1/10; 1/7; and 1/5 at $\lambda = 5$; 1.2; 0.75; and $0.5\,\mu$m, respectively). Below we shall suppose that conditions for applicability of relation (7) are fulfilled.

## 3. Dispersion equations and waveguide solutions for a two-layered plate

Thus, the four unknown amplitudes $A_j^{\pm}$ in (3) can be found from conditions (6), (7) at the interface ($y = 0$) and the surfaces ($y = d_1$ and $y = -d_2$). These conditions provide for each wave family, $TE$ and $TM$, a system of four linear homogeneous equations. The latter systems may have nontrivial solutions only if the corresponding determinants of their coefficients vanish, what leads to appropriate dispersion equations. Of course, they could be also derived by other methods [4,5] or by limiting transition in more general equation [2,3]. Omitting derivations we shall present only final results. For the $TE$ and $TM$ modes, the dispersion equations are respectively given by

$$\tan(kd_1p_1)\cot(kd_2p_2) + p_1/p_2 = 0, \tag{8}$$

$$\tan(kd_1p_1)\cot(kd_2p_2) + \varepsilon_1 p_2/\varepsilon_2 p_1 = 0. \tag{9}$$

The electromagnetic waveguide solution for the $TE$ mode family is determined by the following nonvanishing components:

$$\begin{bmatrix} H_x(y) \\ H_y(y) \\ E_z(y) \end{bmatrix}^{TE} = A \begin{cases} \mathbf{F}_1^{TE}(y)\sin(kd_2p_2), & 0 \le y \le d_1, \\ \mathbf{F}_2^{TE}(y)\sin(kd_1p_1), & -d_2 \le y \le 0; \end{cases} \tag{10}$$

where $A$ is an arbitrary amplitude and

$$\mathbf{F}_1^{TE}(y) = \begin{bmatrix} p_1\cos[kp_1(d_1-y)] \\ i\sin[kp_1(d_1-y)] \\ -i(v/c)\sin[kp_1(d_1-y)] \end{bmatrix},$$

$$\mathbf{F}_2^{TE}(y) = \begin{bmatrix} -p_2\cos[kp_2(y+d_2)] \\ i\sin[kp_2(y+d_2)] \\ -i(v/c)\sin[kp_2(y+d_2)] \end{bmatrix}. \tag{11}$$

Note in passing that at $v$ close to $c_1$ or $c_2$ when the corresponding $p_j \to 0$ certainly there is no physical reasons for vanishing fields in (10), (11). One should just choose in (10) $A \propto 1/p_1p_2$. Similarly, in dispersion equation (8) $p_1 = 0$ is an inadmissible root.

For the $TM$ mode family one similarly obtains

$$\begin{bmatrix} E_x(y) \\ E_y(y) \\ H_z(y) \end{bmatrix}^{TM} = A \begin{cases} \mathbf{F}_1^{TM}(y)\cos(kd_2p_2), & 0 \le y \le d_1, \\ \mathbf{F}_2^{TM}(y)\cos(kd_1p_1), & -d_2 \le y \le 0; \end{cases} \tag{12}$$

with

$$\mathbf{F}_1^{TM}(y) = \begin{bmatrix} ip_1\varepsilon_1^{-1}\sin[kp_1(d_1-y)] \\ \varepsilon_1^{-1}\cos[kp_1(d_1-y)] \\ (v/c)\cos[kp_1(d_1-y)] \end{bmatrix},$$

$$\mathbf{F}_2^{TM}(y) = \begin{bmatrix} -ip_2\varepsilon_2^{-1}\sin[kp_2(y+d_2)] \\ \varepsilon_2^{-1}\cos[kp_2(y+d_2)] \\ (v/c)\cos[kp_2(y+d_2)] \end{bmatrix}. \tag{13}$$

## 4. Dispersion anomalies in the spectrum of a two-layered waveguide

Of course, the presented transcendental dispersion equations (8), (9) cannot be solved analytically. However, as we shall see, many important features of their solutions may be established basing on the idea of some discretization, which was first introduced by Mindlin [13] in his theory of acoustic Lamb waves in a homogeneous elastic plate. For further convenience let us start with some rearranging of the above dispersion equations. We replace there the variables $v$, $k$ by the following dimensionless quantities: the slowness $S = c/v$ and the frequency $f = \omega d/2\pi c$, where $d = d_1 + d_2$ is the thickness of the plate. In these terms

$$kd_j = \omega d_j/v = 2\pi\alpha_j f S, \quad p_j = q_j/S, \quad q_j = \sqrt{N_j^2 - S^2}, \tag{14}$$

where $\alpha_j = d_j/d$ is the dimensionless thickness of the layer $j$, and we remind the reader that $N_j = \sqrt{\varepsilon_j}$ is the refractive index of the layer $j$. Thus, in any further analysis we shall operate with dispersion equations in the form

$$\Phi^{TE}(S, f) \equiv \cos[2\pi\alpha_1 q_1(S) f]\sin[2\pi\alpha_2 q_2(S) f] + (q_2/q_1)\sin[2\pi\alpha_1 q_1(S) f]\cos[2\pi\alpha_2 q_2(S) f] = 0, \tag{15}$$

$$\Phi^{TM}(S, f) \equiv \cos[2\pi\alpha_1 q_1(S) f]\sin[2\pi\alpha_2 q_2(S) f] + (\varepsilon_2 q_1/\varepsilon_1 q_2)\sin[2\pi\alpha_1 q_1(S) f]\cos[2\pi\alpha_2 q_2(S) f] = 0. \tag{16}$$

It is easily seen that both Eq. (15) and (16) are satisfied in an infinite series of points where simultaneously either

$$\sin[2\pi\alpha_1 q_1(S) f] = 0, \tag{17a}$$

$$\sin[2\pi\alpha_2 q_2(S) f] = 0; \tag{17b}$$

or

$$\cos[2\pi\alpha_1 q_1(S) f] = 0, \tag{18a}$$

$$\cos[2\pi\alpha_2 q_2(S) f] = 0. \tag{18b}$$

It can be easily checked (e. g., by some limiting transitions in (15), (16)) that all solutions of Eqs. (17a) and (18a) describe the spectrum of electromagnetic waveguide eigenmodes in a homogeneous plate of the thickness $2d_1$ with the electric permittivity $\varepsilon_1$ and metallized surfaces. These solutions are given by

$$2\pi\alpha_1 q_1(S) f = \frac{\pi}{2} n, \tag{19}$$

which for even $n = 2l$ ($l = 1, 2, \ldots$) satisfies Eq. (17a) and for odd $n = 2r + 1$ ($r = 0, 1, 2, \ldots$) fits Eq. (18a). Quite similarly, all solutions of equations (17b) and (18b) describe the spectrum of a homogeneous dielectric plate with the permittivity $\varepsilon_2$ and the thickness $2d_2$. They are given by

$$2\pi\alpha_2 q_2(S) f = \frac{\pi}{2} m. \tag{20}$$

Again for even $m = 2s$ ($s = 1, 2, \ldots$) (20) is a solution on (17b), and for odd $m = 2t + 1$ ($t = 0, 1, 2, \ldots$) (20) solves (18b).

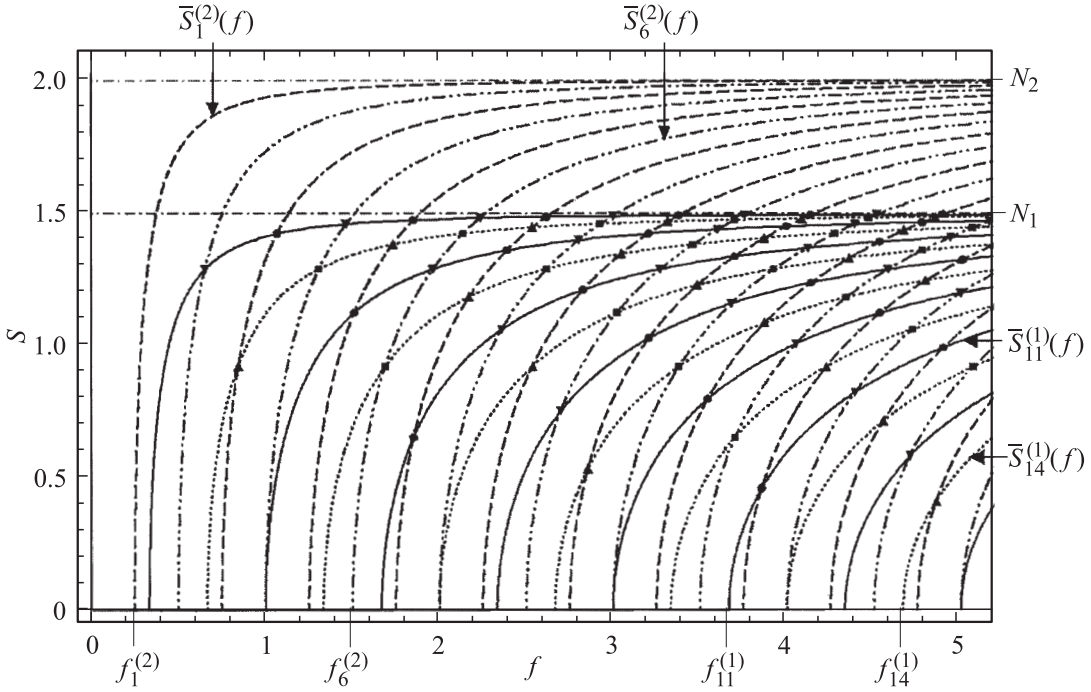


**Figure 2.** Two series of crossing bond lines, $S = \overline{S}_n^{(1)}(f)$ and $S = \overline{S}_m^{(2)}(f)$ (Eq. (21)). Circle and square points coreespond to intersections of odd-odd and even-even bonds, respectively. Triangle up and down points indicate intersections of even-odd and odd-even bonds. In computations, the following parameters were used: $\alpha_1 = \alpha_2 = 0.5$; $N_1 = 1.5$, $N_2 = 2$.

Strictly speaking, after the limiting transition in (15), (16) to homogeneity ($\alpha_2 \to 0$, $\alpha_1 \to 1$) one obtains not exactly Eq. (17a), but this with an additional factor in the left-hand side equal to $q_1^{-1}$ for $TE$ waves and to $q_1$ for $TM$ waves. Accordingly, in the $TM$ spectrum the additional branch $S = N_1$ arises as a solution of the equation $q_1(S) = 0$. This solution describing a one partial bulk polariton satisfying the boundary conditions does not belong to the waveguide spectrum. As we shall see, for an inhomogeneous plate the above branch transforms into a function $S(f)$ which remains finite at $f \to 0$. However in this paper we are more interested in the waveguide modes.

Eqs. (19), (20) with (14) define the two infinite systems of monotonously increasing curves, $S = \overline{S}_n^{(1)}(f)$ and $S = \overline{S}_m^{(2)}(f)$,

$$\overline{S}_n^{(1)}(f) = \sqrt{N_1^2 - \left(\frac{n}{4\alpha_1 f}\right)^2},$$

$$\overline{S}_m^{(2)}(f) = \sqrt{N_2^2 - \left(\frac{m}{4\alpha_2 f}\right)^2}. \qquad (21)$$

Each of these curves starts from the corresponding cutoff frequency:

$$f_n^{(1)} = \frac{n}{4\alpha_1 N_1}, \quad f_m^{(2)} = \frac{m}{4\alpha_2 N_2}, \quad n, m = 1, 2, \ldots, \quad (22)$$

where it vanishes. At $f \to \infty$ they tend to the common asymptotic levels $N_1$ or $N_2$, respectively. We remember that with the initial choice $\varepsilon_1 < \varepsilon_2$, certainly also $N_1 < N_2$. The two infinite sets of lines (21) are analogous to Mindlin's bond lines [13]. Under the level $N_1$ these lines form multiple crossings (the bond grid) with density, which increases for large frequencies $f$ and close to the asymptote $N_1$ (Fig. 2).

Thus, the dispersion lines $S = S_l^{TE}(f)$ and $S = S_l^{TM}(f)$ determined by Eqs. (15), (16), must go throuhg the same nodes $(f_{mn}, S_{mn})$ of the bond grid which correspond to pairs $m, n$ with coinciding evenness. And beyond these nodes the dispersion curves $S_l^{TE}(f)$ and $S_l^{TM}(f)$ may not cross any bond lines. That follows from the comparison of Eqs. (15), (16) with systems (17), (18). And as is seen from Fig. 2, even-even and odd-odd nodes of the grid must be situated along each dispersion curve in succession. Let us find the slopes of the lines $S = S_l^{TE}(f)$ and $S = S_l^{TM}(f)$ in such neighboring nodes. Combining the standard formulae

$$\frac{\partial S_l^{TE}}{\partial f} = -\frac{\partial_f \Phi^{TE}(S, f)}{\partial_S \Phi^{TE}(S, f)}, \quad \frac{\partial S_l^{TM}}{\partial f} = -\frac{\partial_f \Phi^{TM}(S, f)}{\partial_S \Phi^{TM}(S, f)} \quad (23)$$

with explicit forms (15), (16) of the functions $\Phi^{TE}(S, f)$ and $\Phi^{TM}(S, f)$ we find

$$\left.\frac{\partial S_l^{TE}}{\partial f}\right|_{\substack{n=2r \\ m=2s}} = \frac{1}{f_{mn} S_{mn} \left(\frac{\alpha_1}{q_1^2(S_{mn})} + \frac{\alpha_2}{q_2^2(S_{mn})}\right)},$$

$$\left.\frac{\partial S_l^{TM}}{\partial f}\right|_{\substack{n=2r \\ m=2s}} = \frac{1}{f_{mn} S_{mn}} \frac{\alpha_1 \varepsilon_2 q_1^2(S_{mn}) + \alpha_2 \varepsilon_1 q_2^2(S_{mn})}{\alpha_1 \varepsilon_2 + \alpha_2 \varepsilon_1}, \quad (24a)$$

$$\left.\frac{\partial S_l^{TE}}{\partial f}\right|_{\substack{n=2r+1\\m=2s+1}} = \frac{\alpha_1 q_1^2(S_{mn}) + \alpha_2 q_2^2(S_{mn})}{f_{mn} S_{mn}},$$

$$\left.\frac{\partial S_l^{TM}}{\partial f}\right|_{\substack{n=2r+1\\m=2s+1}} = \frac{\alpha_1 \varepsilon_1 + \alpha_2 \varepsilon_2}{f_{mn} S_{mn}\left(\frac{\alpha_1 \varepsilon_1}{q_1^2(S_{mn})} + \frac{\alpha_2 \varepsilon_2}{q_2^2(S_{mn})}\right)}. \qquad (24b)$$

Thus, the slopes of the dispersion curves $S = S_l^{TE}(f)$ and $S = S_l^{TE}(f)$ are essentially different both for each line in the neighboring nodes of the bond grid and for the two these lines in the same nodes of the grid. With this observation we can predict a wavy („zigzag“) character of the two families of dispersion curves inside the zone occupied by the bond grid (Fig. 2). The waviness must be more pronounced at large frequencies in the vicinity of the level $S = N_1$ where the density of the grid is increasing and the distance between neighboring nodes accordingly becomes less and less. Note in addition that in nodes situated close to the level $N_1$ the parameter $q_1$ tends to zero and the ratios of appropriate derivatives in (24) tend to infinity.

Beyond the grid zone, we would expect for dispersion curves a rather smooth behavior between appropriate bond lines. At the zero level $S = 0$, they should start in some cutoff frequencies situated between some points (22) and determined by Eqs. (15), (16) where one must put $q_j = N_j$. It is essential that at this level the two equations identically coincide because at $q_j = N_j$ one obtains $q_2/q_1 = \varepsilon_2/q_1/\varepsilon_1 q_2 = \sqrt{\varepsilon_2/\varepsilon_1}$. Accordingly the cutoff frequency spectra for both branches $TE$ and $TM$ prove to be identical, and the curves $S_l^{TE}(f)$ and $S_l^{TM}(f)$ must start at $S = 0$ in the same points. One can check that derivatives (23) at these points are proportional to $1/S$ and tend to infinity when $S \to 0$, i.e. all dispersion curves start vertically. This and all the other above expectations are corroborated by a numerical solution of Eqs. (15), (16) (see Fig. 3).

Let us find the crossing points of the dispersion curves $S = S_l^{TE}(f)$ and $S = S_l^{TM}(f)$ with the level $S = N_1$ where by definition (14) $q_1 = 0$. The first series of points $f_l^{TE}$ is determined by Eq. (15) after its limiting transformation $q_1 \to 0$:

$$\cot[2\pi\alpha_2 q_2(N_1) f] = -1/2\pi\alpha_1 q_2(N_1) f. \qquad (25)$$

It is easily deduced that roots $f_l^{TE}$ of this transcendental equation lie between the crossing points of the bond lines $\bar{S}_{2l-1}^{(2)}(f)$ and $\bar{S}_{2l}^{(2)}(f)$ with the same level $S = N_1$. For increasing number $l$, i.e. with growth of frequency $f$, when the right-hand side in (25) is tending to zero, the solutions of (25) $f_l^{TE}$ must be closing from the right to the intersection points of $\bar{S}_{2l-1}^{(2)}(f)$ with the level $N_1$ where

$$2\pi\alpha_2 q_2(N_1) f = \frac{\pi}{2}(2l-1), \qquad (26)$$

see the black circles at the level $N_1$ in Fig. 3.

The second series of crossing points $f_l^{TM}$ determined by the equation $S_l^{TM}(f) = N_1$, in view of Eq. (16) taken at $q_1(N_1) = 0$, is reduced to

$$\sin[2\pi\alpha_2 q_2(N_1) f] = 0, \quad 2\pi\alpha_2 q_2(N_1) f = \frac{\pi}{2} 2l. \qquad (27)$$

Thus the points $f_l^{TM}$ where the dispersion curves $S_l^{TM}(f)$ intersect the line $S = N_1$ must coincide with crossing points of the bond lines $\bar{S}_{2l}^{(2)}(f)$ with the same level $N_1$ (see the square points in Fig. 3).

Basing on (23) one can also find slopes of the dispersion functions $S_l^{TE}(f)$ and $S_l^{TM}(f)$ in their crossing points $f_l^{TE}$ and $f_l^{TM}$ with the level $N_1$:

$$\left.\frac{\partial S_l^{TE}}{\partial f}\right|_{S=N_1} = \frac{N_1(\varepsilon_2 - \varepsilon_1)}{f_1^{TE}} \frac{1 + \alpha_2 (2\pi\alpha_1 f_l^{TE})^2 (\varepsilon_2 - \varepsilon_1)}{1 + (2\pi\alpha_1 f_l^{TE})^2 (\varepsilon_2 - \varepsilon_1)}, \qquad (28)$$

$$\left.\frac{\partial S_l^{TM}}{\partial f}\right|_{S=N_1} = \frac{N_1}{f_l^{TM}} \frac{\varepsilon_2 - \varepsilon_1}{1 + 2\alpha_1\varepsilon_2/\alpha_2\varepsilon_1}. \qquad (29)$$

The important common feature of the found derivatives is their vanishing in the limit $l \to \infty$ (i.e. $f \to \infty$), which reflects a very specific asymptotic behavior of dispersion curves of the two families at the level $S = N_1$. They form a sort of step-like terracing pattern closing to the asymptote $S = N_1$ in succession one by one changing each other in the lower vicinity of this level. And each next dispersion line comes closer to the asymptote than its predecessor but then intersects the asymptote at the points $f_l^{TE}$ or $f_l^{TM}$ and goes up to the other asymptote $S = N_2$. Fig. 3 illustrates this important feature of the studied spectra.

As follows from the above consideration and Fig. 3, *a*, the dispersion branches $S_l^{TE}(f)$ and $S_l^{TM}(f)$ above the level $S = N_1$ go up between the appropriate bond lines,

$$\bar{S}_{2l+1}^{(2)}(f) < S_l^{TM}(f) < \bar{S}_{2l}^{(2)}(f) < S_l^{TE}(f) < \bar{S}_{2l-1}^{(2)}(f), \qquad (30)$$

and together with them smoothly tend to the asymptote $S = N_2$. Taking into account that for $S > N_1$ the parameter $q_1(S)$ (14) becomes purely imaginary it is convenient to replace it by the real parameter substituting into (15), (16) $q_1 = i\bar{q}_1$, where

$$\bar{q}_1 = \sqrt{S^2 - N_1^2}, \qquad (31)$$

and simultaneously $\sin(2\pi\alpha_1 q_1 f) \to i\sinh(2\pi\alpha_1 \bar{q}_1 f)$, $\cos(2\pi\alpha_1 q_1 f) \to \cosh(2\pi\alpha_1 \bar{q}_1 f)$. As a result, for $S > N_1$ dispersion equations (15), (16) respectively acquire the other form:

$$\tan(2\pi\alpha_2 q_2 f) = -\frac{q_2}{\bar{q}_1} \tanh(2\pi\alpha_1 \bar{q}_1 f), \qquad (32)$$

$$\tan(2\pi\alpha_2 q_2 f) = \frac{\varepsilon_2 \bar{q}_1}{\varepsilon_1 q_2} \tanh(2\pi\alpha_1 \bar{q}_1 f), \qquad (33)$$

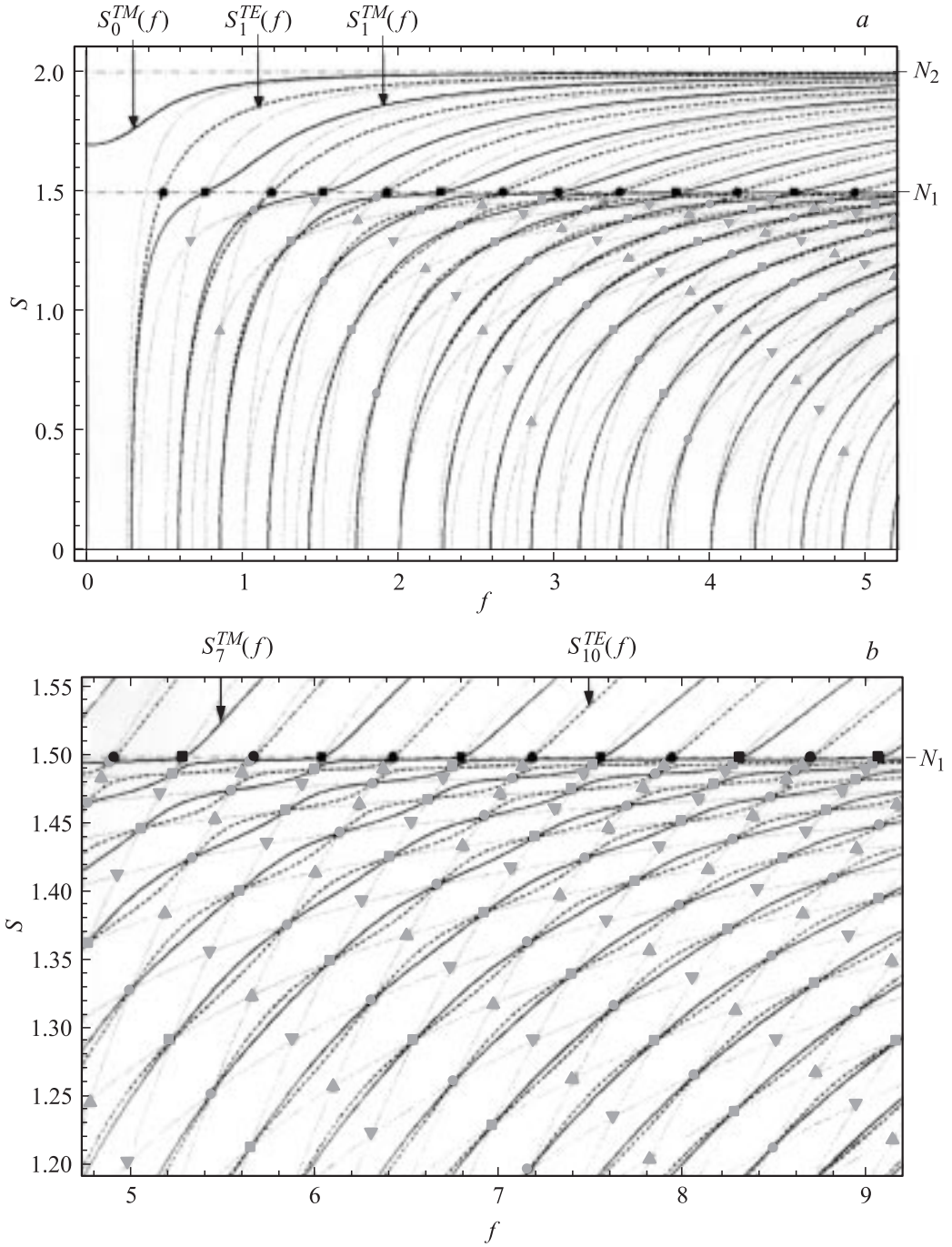


**Figure 3.** Numerical plot of dispersion curves $S = S_l^{TE}(f)$ and $S = S_l^{TM}(f)$ on the background of bonds $S = \bar{S}_n^{(1)}(f)$ and $S = \bar{S}_l^{(2)}(f)$ (grey lines) for a small scale ($a$) and for a large scale image of the high frequency part ($b$). The used parameters are the same as in Fig. 2.

Eq. (32) describes the dispersion branches $S = S_l^{TE}(f)$ and for large $f$ (when $S \to N_2$ and $q_2 \to 0$) tends to the form of Eq. (17b). This shows that with increase of the frequency $f$ the curves $S_l^{TE}(f)$ must approach from above the bond lines $\bar{S}_{2l}^{(2)}(f)$. Quite similarly, Eq. (33) in the same limit transforms to the form (18b) and the corresponding dispersion branches $S_l^{TM}(f)$ will tend from above to the bond lines $\bar{S}_{2l+1}^{(2)}(f)$ with their further common approaching the asymptotic level $S = N_2$.

The numerical results, shown in Fig. 3, $a$, completely fit analytically deduced features. In additon, as was expected, the $TM$ spectrum proves to contain the additional upper mode $S_0^{TM}(f) > \bar{S}_1^{(2)}(f)$ completely belonging to the region $N_1 < S < N_2$ and related to the fundamental eigenmode not associating with the waveguide spectrum. Its principal distinction from the waveguide series consists in different behavior at small $f$: the function $S_0^{TM}(f)$ does not vanish at $f = 0$ but, as follows from (16), it is coming horizontally

out the point (Fig. 3, $a$)

$$S_0^{TM}(0) = \sqrt{\frac{\varepsilon_1\varepsilon_2}{\alpha_1\varepsilon_2 + \alpha_2\varepsilon_1}} = \frac{N_1}{\sqrt{1-\alpha_2(1-\varepsilon_1/\varepsilon_2)}} > N_1.$$

## 5. Symmetric three-layered waveguide

Let us now consider a three-layered sandwich structure as shown in Fig. 1, $b$. This symmetric waveguide is supposed to be made of the same two isotropic materials as the above studied two-layered plate. Thus, here in additon to the symmetry plane coinciding with the sagittal plane $xy$ of wave propagation we acquire the other symmetry plane situated in the central $xz$ plane. Therefore in the given case we should deal with four independent eigenwave families, because now each of the $TE$ and $TM$ wave series will split into symmetric and antisymmetric familites: $TE \to (TE)_{S,A}$ and $TM \to (TM)_{S,A}$. Of course, just as before, the terminology is conventional: for instance, in the $(TE)_S$ modes the symmetric transverse electric field is accompanied by the antisymmetric in-plane magnetic field, and in the $(TM)_A$ family the antisymmetric transverse magnetic field coexists with the symmetric in-plane electric field (Fig. 4).

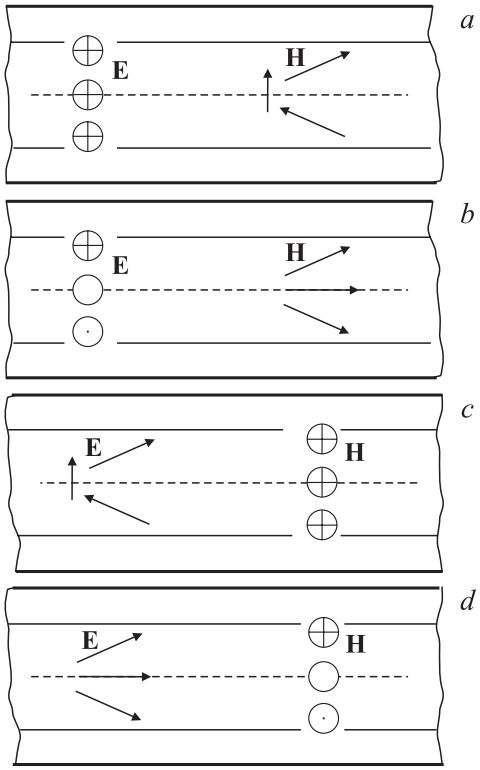


**Figure 4.** The four independent eigenwave families for a symmetric three-layered structure. $a$ — modes $(TE)_S$: symmetric electric field $\mathbf{E} \parallel z$ and antisymmetric magnetic field $\mathbf{H} \perp z$, $b$ — modes $(TE)_A$: antisymmetric electric field $\mathbf{E} \parallel z$ and symmetric magnetic field $\mathbf{H} \perp z$, $c$ — modes $(TM)_S$: symmetric magnetic field $\mathbf{H} \parallel z$ and antisymmetric electric field $\mathbf{E} \perp z$, $d$ — modes $(TM)_A$: antisymmetric magnetic field $\mathbf{H} \parallel z$ and symmetric electric field $\mathbf{E} \perp z$.

Mathematically an analysis of this problem is completely similar to our consideration for the case of a two-layered plate. Accordingly, we shall not repeat derivations and just present the results. The steady-state form (2) for the waveguide electromagnetic fields certainly remains valid. And the structure of amplitudes $[\mathbf{E}(y), \mathbf{H}(y)]$ for all independent eigenwave families in the coordinate system specified by Fig. 1, $b$ has the following forms. For the $(TE)_S$ famili:

$$\begin{bmatrix} H_x(y) \\ H_y(y) \\ E_z(y) \end{bmatrix}^{(TE)_S} = A \begin{cases} \mathbf{F}_1^{(TE)_S}(y)\cos(kd_1p_1), & d_1 \le y \le d; \\ \mathbf{F}_2^{(TE)_S}(y)\sin(kd_2p_2), & -d_1 \le y \le d_1; \\ \mathbf{F}_3^{(TE)_S}(y)\cos(kd_1p_1), & -d \le y \le -d_1; \end{cases} \tag{34}$$

where, as before, $d = d_1 + d_2$ and

$$\mathbf{F}_1^{(TE)_S} = \begin{bmatrix} -p_2\cos[kp_2(d-y)] \\ -i\sin[kp_2(d-y)] \\ i\frac{v}{c}\sin[kp_2(d-y)] \end{bmatrix},$$

$$\mathbf{F}_2^{(TE)_S} = \begin{bmatrix} -p_1\sin(kp_1y) \\ -i\cos(kp_1y) \\ i\frac{v}{c}\cos(kp_1y) \end{bmatrix},$$

$$\mathbf{F}_3^{(TE)_S} = \begin{bmatrix} p_2\cos[kp_2(d+y)] \\ -i\sin[kp_2(d+y)] \\ i\frac{v}{c}\sin[kp_2(d+y)] \end{bmatrix}. \tag{35}$$

And similarly for the other families:

$$\begin{bmatrix} H_x(y) \\ H_y(y) \\ E_z(y) \end{bmatrix}^{(TE)_A} = A \begin{cases} \mathbf{F}_1^{(TE)_A}(y)\sin(kd_1p_1), & d_1 \le y \le d; \\ \mathbf{F}_2^{(TE)_A}(y)\sin(kd_2p_2), & -d_1 \le y \le d_1; \\ \mathbf{F}_3^{(TE)_A}(y)\sin(kd_1p_1), & -d \le y \le -d_1; \end{cases} \tag{36}$$

$$\mathbf{F}_1^{(TE)_A} = \begin{bmatrix} -p_2\cos[kp_2(d-y)] \\ -i\sin[kp_2(d-y)] \\ i\frac{v}{c}\sin[kp_2(d-y)] \end{bmatrix},$$

$$\mathbf{F}_2^{(TE)_A} = \begin{bmatrix} p_1\cos(kp_1y) \\ -i\sin(kp_1y) \\ i\frac{v}{c}\sin(kp_1y) \end{bmatrix},$$

$$\mathbf{F}_3^{(TE)_A} = \begin{bmatrix} -p_2\cos[kp_2(d+y)] \\ i\sin[kp_2(d+y)] \\ -i\frac{v}{c}\sin[kp_2(d+y)] \end{bmatrix}; \tag{37}$$

$$\begin{bmatrix} E_x(y) \\ E_y(y) \\ H_z(y) \end{bmatrix}^{(TM)_S} = A \begin{cases} \mathbf{F}_1^{(TM)_S}(y)\cos(kd_1p_1), & d_1 \le y \le d; \\ \mathbf{F}_2^{(TM)_S}(y)\cos(kd_2p_2), & -d_1 \le y \le d_1; \\ \mathbf{F}_3^{(TM)_S}(y)\cos(kd_1p_1), & -d \le y \le -d_1; \end{cases} \tag{38}$$

$$\mathbf{F}_1^{(TM)_S} = \begin{bmatrix} i\frac{p_2}{\varepsilon_2}\sin[kp_2(d-y)] \\ \frac{1}{\varepsilon_2}\cos[kp_2(d-y)] \\ \frac{v}{c}\cos[kp_2(d-y)] \end{bmatrix},$$

$$\mathbf{F}_2^{(TM)_S} = \begin{bmatrix} -i\frac{p_1}{\varepsilon_1}\sin(kp_1y) \\ \frac{1}{\varepsilon_1}\cos(kp_1y) \\ \frac{v}{c}\cos(kp_1y) \end{bmatrix},$$

$$\mathbf{F}_3^{(TM)_S} = \begin{bmatrix} -i\frac{p_2}{\varepsilon_2}\sin[kp_2(d+y)] \\ \frac{1}{\varepsilon_2}\cos[kp_2(d+y)] \\ \frac{v}{c}\cos[kp_2(d+y)] \end{bmatrix}; \tag{39}$$

$$\begin{bmatrix} E_x(y) \\ E_y(y) \\ H_z(y) \end{bmatrix}^{(TM)_A} = A \begin{cases} \mathbf{F}_1^{(TM)_A}(y)\sin(kd_1p_1), & d_1 \le y \le d; \\ \mathbf{F}_2^{(TM)_A}(y)\cos(kd_2p_2), & -d_1 \le y \le d_1; \\ \mathbf{F}_3^{(TM)_A}(y)\sin(kd_1p_1), & -d \le y \le -d_1; \end{cases} \tag{40}$$

$$\mathbf{F}_1^{(TM)_A} = \begin{bmatrix} i\frac{p_2}{\varepsilon_2}\sin[kp_2(d-y)] \\ \frac{1}{\varepsilon_2}\cos[kp_2(d-y)] \\ \frac{v}{c}\cos[kp_2(d-y)] \end{bmatrix},$$

$$\mathbf{F}_2^{(TM)_A} = \begin{bmatrix} i\frac{p_1}{\varepsilon_1}\cos(kp_1y) \\ \frac{1}{\varepsilon_1}\sin(kp_1y) \\ \frac{v}{c}\sin(kp_1y) \end{bmatrix},$$

$$\mathbf{F}_3^{(TM)_A} = \begin{bmatrix} i\frac{p_2}{\varepsilon_2}\sin[kp_2(d+y)] \\ -\frac{1}{\varepsilon_2}\cos[kp_2(d+y)] \\ -\frac{v}{c}\cos[kp_2(d+y)] \end{bmatrix}. \tag{41}$$

In all cases the continuity condition for the $x$-components of the fields $\mathbf{E}(y)$ and $\mathbf{H}(y)$ at the interfaces $y = \pm d_1$ provides appropriate dispersion equations (boundary conditions (7) are satisfied automatically). It is easily checked that these equations are

$$\Phi_S^{TE}(S, f) \equiv \cot[2\pi\alpha_1 q_1(S) f]\cot[2\pi\alpha_2 q_2(S) f] - q_1/q_2 = 0, \tag{42}$$

$$\Phi_A^{TE}(S, f) = \tan[2\pi\alpha_1 q_1(S) f]\cot[2\pi\alpha_2 q_2(S) f] + q_1/q_2 = 0, \tag{43}$$

$$\Phi_S^{TM}(S, f) = \tan[2\pi\alpha_1 q_1(S) f]\cot[2\pi\alpha_2 q_2(S) f] + \varepsilon_1 q_2/\varepsilon_2 q_1 = 0, \tag{44}$$

$$\Phi_A^{TM}(S, f) = \cot[2\pi\alpha_1 q_1(S) f]\cot[2\pi\alpha_2 q_2(S) f] - \varepsilon_1 q_2/\varepsilon_2 q_1 = 0. \tag{45}$$

As is seen from Eqs. (36)–(39), the wave systems $(TE)_A$ and $(TM)_S$ formally satisty the boundary condition (7) at $y = 0$. Therefore, it is natural that Eqs. (43) and (44) actually coincide with already studied dispersion equations (8) and (9), respectively, for a two-layered plate. Such relations between boundary problems for two- and symmetrical three-layered waveguides are known both in optics and in acoustics [12]. Additional equations (42) and (45) can be analyzed in a completely similar manner. The corresponding dispersion curves $S_l^{(TE)_S}(f)$ and $S_l^{(TM)_A}(f)$ also must start vertically in the coinciding cutoff frequencies, which are however different from those for the branches $S_l^{(TE)_A}(f)$ and $S_l^{(TM)_S}(f)$. Then they go through the nodes of the same bond grid, however this time through the other nodes formed by intersection points of the even bond lines $\overline{S}_{2r}^{(1)}(f)$ with the odd bond lines $\overline{S}_{2s+1}^{(2)}(f)$ and by crossings of the lines $\overline{S}_{2r+1}^{(1)}(f)$ and $\overline{S}_{2s}^{(2)}(f)$. Bearing in mind that the pairs of dispersion curves $S_l^{(TE)_S}(f)$, $S_l^{(TM)_A}(f)$ and $S_l^{(TE)_A}(f)$, $S_l^{(TM)_S}(f)$ go through different nodes of the grid and cannot intersect bond lines, we arrive at the conclusion that there are no intersections between these pairs, only inside of them. Crossing each other in the mentioned nodes of the grid, the additional dispersion branches must be also wavy in the grid zone and smooth beyond it. All these features one can see in Fig. 5.

In the vicinity of the level $S = N_1$, a step-like terracing pattern again occurs for these branches. One can easily deduce from Eq. (42) that the dispersion curves of the family $(TE)_S$ cross the level $N_1$ at the points where Eq. (18b) is satisfied, i.e. where the bond lines $\overline{S}_{2l-1}^{(2)}(f)$ do it (the white square points in Fig. 5). Thus the branches $S_l^{(TE)_S}(f)$ must go up to the asymptote $S = N_2$ between the bond lines:

$$\overline{S}_{2l}^{(2)}(f) < S_l^{(TE)_S}(f) < \overline{S}_{2l-1}^{(2)}(f). \tag{46}$$

It also follows from (42) that these branches at large $f$ become close to the left limit in (46):

$$S_l^{(TE)_S}(f) \approx \overline{S}_{2l}^{(2)}(f), \tag{47}$$

which is the same as for the branch $S_l^{(TE)_A}(f)$ (see Fig. 5, *a*).

Quite similarly one can conclude from Eq. (45) that the crossing points of the dispersion curves $S_l^{(TM)_A}(f)$ with the level $N_1$ are determined by the following equation

$$\tan[2\pi\alpha_2 q_2(N_1) f] = 1/2\pi\alpha_1 q_2(N_1) f, \tag{48}$$

which is analogous to (25). This equation shows that the desired crossing points take place between those for

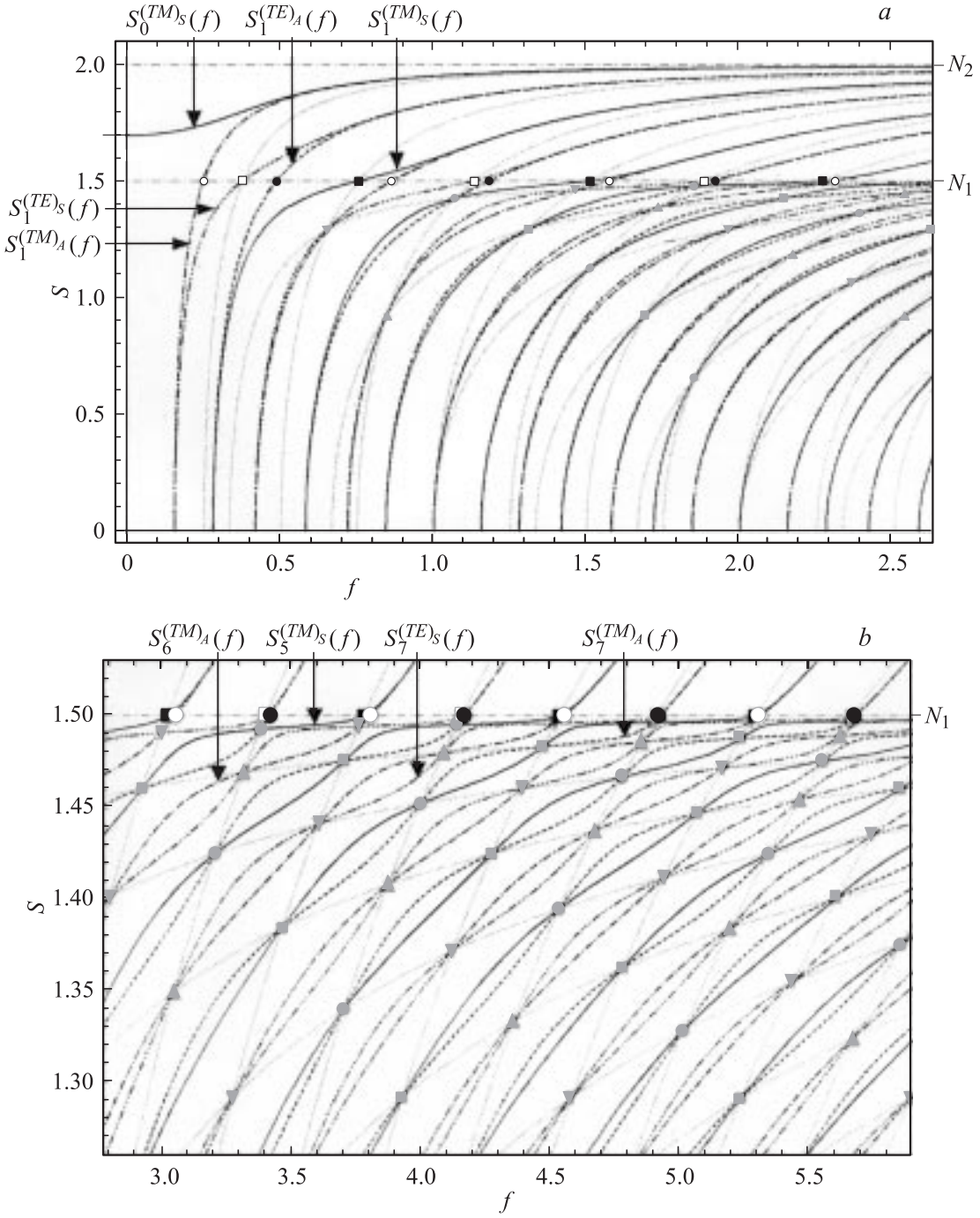


**Figure 5.** Spectra of symmetric and antisymmetric waves $(TE)_S$, $(TE)_A$, $(TM)_S$ and $(TM)_A$ in the three-layered plate shown in Fig. 4 for small ($a$) and large ($b$) scale images in the slowness $S$ and for different ranges of the frequency $f$. Parameters are the same as in Fig. 2.

the bond lines $\overline{S}_{2l-1}^{(2)}(f)$ and $\overline{S}_{2l-2}^{(2)}(f)$ tending to the left limit when $f \to \infty$ (see the white round points in Fig. 5). Above $N_1$ the branches $S_l^{(TM)_A}(f)$ naturally remian between the same bond lines and at large $f$ they must be close to the lower bonds:

$$S_l^{(TM)_A}(f) \approx \overline{S}_{2l-1}^{(2)}(f), \tag{49}$$

i. e. to the same bonds as $S_{l-1}^{(TM)_S}(f)$, see Fig. 5.

Thus, as follows from the above considerations and Fig. 5, the dispersion lines $S_l^{(TE)_S}(f)$ and $S_l^{(TE)_A}(f)$ tend with increasing $f$ to the same limiting bond $\overline{S}_{2l}^{(2)}(f)$. And similarly, the pair $S_l^{(TM)_A}(f)$ and $S_{l-1}^{(TM)_S}(f)$ tends to $\overline{S}_{2l-1}^{(2)}(f)$. However, one can easily check that intersections between these pairs are forbidden. The reason for that becomes clear if we present the dispersion equations, say (42) and (43), in the form natural for this region

[see Eqs. (32), (33)]:

$$\tan(2\pi\alpha_2 q_2 f) = -\frac{q_2}{\bar{q}_1}\coth(2\pi\alpha_1\bar{q}_1 f), \qquad (50)$$

$$\tan(2\pi\alpha_2 q_2 f) = -\frac{q_2}{\bar{q}_1}\tanh(2\pi\alpha_1\bar{q}_1 f). \qquad (51)$$

The similar system arises from analogous operations with Eqs. (44) and (45). Thus, we can see that crossings between the discussed dispersion lines in the considered range are impossible because at any $f$

$$\tanh(2\pi\alpha_1\bar{q}_1 f) < \coth(2\pi\alpha_1\bar{q}_1 f). \qquad (52)$$

On the other hand, it is evident that for sufficiently large argument $2\pi\alpha_1\bar{q}_1 f$ the right and left hand-sides of inequality (52) differ by only exponentially small terms $\sim \exp(-2\pi\alpha_1\bar{q}_1 f)$. This explains why in Fig. 5 at sufficiently large $f$ the above pairs of dispersion cureves are almost indistinguishable just after the intersection of the level $N_1$.

Thus, we can state that in our spectra crossings of the dispersion lines are possible only below the first asymptote $S = N_1$ in the appropriate nodes of the bond grid.

## 6. Extensions to anisotropy

The above presented considerations that are related to waveguides composed of isotropic layers (Fig. 1), can be easily extended taking account of some anisotropy, when all isotropic materials of the layers are replaced by uniaxial crystals with the principal axes orientaion **t** either orthogonal to the sagittal plane ($\mathbf{t} \parallel z$), or parallel to the propagation direction ($\mathbf{t} \parallel x$). Anisotropy brings with itself tensors of electric permittivity $\hat{\varepsilon}_j$ ($j = 1, 2$) instead of scalars $\varepsilon_j$. For instance, if we choose the first variant of crystallographic orientation ($\mathbf{t} \parallel z$) the structure of $\hat{\varepsilon}_j$ is given by [20]:

$$\hat{\varepsilon}_j = \begin{bmatrix} \varepsilon_j^o & 0 & 0 \\ 0 & \varepsilon_j^o & 0 \\ 0 & 0 & \varepsilon_j^e \end{bmatrix}. \qquad (53)$$

We remind the reader that in optics the electric permittivities $\varepsilon^o$ and $\varepsilon^e$ determine the properties of the known ordinary and extraordinary waves in uniaxial crystals.

In crystalline waveguides of the considered type, instead of universal bulk wave speeds (1), one should now distinguish the speeds

$$c_j^{TE} = c/\sqrt{\varepsilon_j^e}, \quad c_j^{TM} = c/\sqrt{\varepsilon_j^o}. \qquad (54)$$

Accordingly, the parameters $p_j$ (5) will also become different for $TE$ and $TM$ modes:

$$p_j^{TE} = \sqrt{(v/c_j^{TE})^2 - 1}, \quad p_j^{TM} = \sqrt{(v/c_j^{TM})^2 - 1}. \qquad (55)$$

As a result, we should replace everywhere the parameters $c_j$, $N_j$, $p_j$ and $q_j$ respectively by $c_j^\alpha$, $N_j^\alpha$, $p_j^\alpha$ and $q_j^\alpha$ with an appropriate choice of $\alpha = TE$ or $TM$.

The most important complication of the above studied spectral picture is related to the bond lines (21) and the resulting bond grid, which used to be universal for all dispersion equations, both for two-layered and for three-layered plates. Now, after replacement in (21) $N_j$ by $N_j^\alpha$ the bond lines become different for $TE$ and $TM$ modes. Accordingly, we obtain two different bond grids for these series of modes, which now go through the definite nodes in their own grids. Thus, the beautiful property of crossing independent branches in nodes of a universal grid is completely destroyed by anisotropy. Even in a three-layered plate, where each of dispersion pairs $S_l^{(TE)_S}(f)$, $S_l^{(TE)_A}(f)$ and $S_l^{(TM)_S}(f)$, $S_l^{(TM)_A}(f)$ shares the same grids, there is no intersections in the nodes of these grids, because, as we have seen, inside of these pairs (belonging to the same grids) there are no crossings. And intersections of the first pair with the second one will occur in points, which are generally situated beyond the nodes of both grids and hardly may be found analytically. We stress that, in contrast to the case of isotropic layers when the branch $S_l^{(TE)_S}(f)$ could cross only the curve $S_l^{(TM)_A}(f)$ (of the same order $l$), and the branch $S_l^{(TE)_A}(f)$ — only the line $S_l^{(TM)_S}(f)$, now we can exclude only intersection inside of these groups ($TE$ and $TM$), otherwise there are no general limitations.

On the other hand, each of the families of dispersion branches individually conserves all their anomalous properties, including terracing at the levels $S = N_j^\alpha$ and a wavy form in the grid zones. And the positions of these dispersion curves in their bond grids are determined by the relations which can be easily established by a trivial extension of those found above.

## 7. Conclusions

As was already mentioned, the established specific features of electromagnetic wave-guide spectra prove to be very similar to spectral peculiarities of analogous acoustical layered structures. Moreover, according to [12], even a form of dispersion equations describing waveguide shear horizontal (SH) acoustic modes in two- and three-layered elastic plates, like shown in Fig. 1, turns out to be very close to equations studied in this paper. For instance, the dispersion equations on SH acoustic modes in a two-layered plate with clamped or free surfaces are respectively given by

$$\tan(kd_1 p_1)\cot(kd_2 p_2) + \mu_1 p_1/\mu_2 p_2 = 0, \qquad (56)$$

$$\tan(kd_1 p_1)\cot(kd_2 p_2) + \mu_2 p_2/\mu_1 p_1 = 0. \qquad (57)$$

Here $\mu_j$ ($j = 1, 2$) are the shear moduli of the corresponding layers, and the parameters $p_j$ are defined by same Eq. (5) where $c_1$ and $c_2$ now stand for the speeds of transverse elastic waves in the layers. One can see that Eq. (56) transforms to (8) at $\mu_1 = \mu_2$, and (57) coincides with (9) after the replacement $\mu_2/\mu_1 \to \varepsilon_1/\varepsilon_2$. In the same way, dispersion equations (42) and (43) describing respectively electromagnetic symmetric and antisymmetric $TE$

modes in three-layered waveguides can be obtained from the corresponding dispersion equations for antisymmetric SH acoustic waves in three-layered plates with free or clamped surfaces. And after similar replacements dispersion equations (44) and (45) for symmetric and antisymmetric $TM$ electromagnetic waves respectively coincide with dispersion equations for symmetric SH acoustic waves in the same three-layered structure with free or clamped faces.

So, the similarity is remarkable but not literal, the more so that, say, Eqs. (8), (9) are the dispersion equations of one eigenwave problem, and (56), (57) solve two different boundary problems. It is worthwhile to emphasize also the other two important consequences of literal distinction between the couples (8), (9) and (56), (57). The first is related to the above established identily of the cutoff frequency spectra for the branches $TE$ and $TM$ for a two-layered waveguide and for the pairs $(TE)_S \,\&\, (TM)_A$ and $(TE)_A \,\&\, (TM)_S$ for a symmetric three-layeres waveguide. One can easily check on the example of Eqs. (56), (57) that the analogous cutoff acoustic spectra are not at all identical.

The other consequence has an opposite effect. As was noticed in [12], the both dispersion equations (56) and (57) become identicall when $\mu_1 p_1 = \mu_2 p_2$, which can be realized at a definite level of the tracing speed $v = v_0$ for an appropriate choice of other parameters. At this level there should occur intersections of the corresponding dispersion branches beyond the nodes of the bond grid. As is seen from (8), (9), such situation for electromagnetic waveguide modes is excluded. Indeed, it could be realized only when

$$\frac{\varepsilon_1 p_2}{\varepsilon_2 p_1} = \frac{p_1}{p_2}, \tag{58}$$

i.e. if the equation $\varepsilon_1 p_2^2 = \varepsilon_2 p_1^2$ may be realized. However, as follows form (5) and (1), the difference $\varepsilon_1 p_2^2 - \varepsilon_2 p_1^2$ in our case may not vanish:

$$\begin{aligned} \varepsilon_1 p_2^2 - \varepsilon_2 p_1^2 &= \varepsilon_1(\varepsilon_2 v^2/c^2 - 1) - \varepsilon_2(\varepsilon_1 v^2/c^2 - 1) \\ &= \varepsilon_2 - \varepsilon_1 \neq 0. \end{aligned} \tag{59}$$

Thus, in electromagnetic waveguides of the considered types (Fig. 1) the dispersion branches may not cross each other beyond nodes of the bond grid.

There is also another important difference of the obtained results for electromagnetic waveguides from their acoustic analogs. In the above consideration we have solved the problem of eigenwave electromagnetic spectrum for layered waveguides in its general statement, i.e. taking into account the modes of all possible polatizations, both transverse and in-plane. And all mentioned acoustic analogs relate only to one possible polarization type of eigenmodes — the transverse (SH) waves. The description of in-plane polartized waveguide acoustic modes in layered plates is a separate problem, which is still waiting for its analytical analysis. Howerver, it is remarkable that the corresponding problem of in-plane polarized Lamb acoustic waves in a homogeneous plate is again described by dispersion equations similar to our Eqs. (8), (9). For a reverse adaptation of these equations to the acoustic case one should put $d_1 = d_2 = d/2$ and interpret $c_1$ and $c_2$ respectively as the speeds of transverse and longitudinal elastic waves in the plate. Then for a plate with free faces Eqs. (8) and (9) will describe respectively antisymmetric and symmetric Lamb waves [21] if there we make the following replacements

$$\frac{p_1}{p_2} \to \frac{(p_1^2 - 1)^2}{4 p_1 p_2}, \quad \frac{\varepsilon_1 p_2}{\varepsilon_2 p_1} \to \frac{4 p_1 p_2}{(p_1^2 - 1)^2}. \tag{60}$$

Quite similarly, for the plate with clamped faces, the dispersion equations for antisymmetric and symmetric waves [22] are obtained from (8) and (9) after the respective renormalization

$$p_1/p_2 \to 1/p_1 p_2, \quad \varepsilon_1 p_2/\varepsilon_2 p_1 \to p_1 p_2. \tag{61}$$

To end with we recall that the concepts used in this paper and in [12] are key concepts of bond lines and bond grid as first introduced by Mindlin [13] in his theory of Lamb waves in elastic plates with free surfaces. Here these concepts prove to be very fruitful.

This work was supported by the Russian Foundation for Basic Research and by the Polish Foundation MNiSW. V.A. acknowledges also a support from the Polish-Japanese Institute of Information Technology, from the Kielce University of Technology, and from the LMP (Bordeaux, France) and the LMM (Paris, France).

## References

[1] Л. Левин. Современная теория волноводов. ИЛ, М. (1954). [L. Lewin. Advanced theory of waveguides. London (1951)].
[2] М. Борн, Э. Вольф. Основы оптики. Наука, М. (1973). [M. Born, E. Wolf. Principles of optics. Pergamon, Oxford (1968)].
[3] А.М. Гончаренко, В.А. Карпенко. Основы теории оптических волноводов. Наука и техника, Минск (1983). [A.M. Goncharenko, V.A. Karpenko. Foundations of the theory of optical waveguides. Nauka i Tekhnika, Minsk (1983) — in Russian].
[4] W.C. Chew. Waves and fields in inhomogenious media. IEEE Press, N.Y. (1995).
[5] L. Felsen, N. Marcuvitz. Radiation and scattering of waves. Wiley, N.Y. (2003).
[6] G.A. Maugin. Proc. 15th Int. Congress of Theoretical & Applied Mechanics. Toronto (1980). In: Theoretical and Applied mechanics. North-Holland, Amsterdam (1980). P. 345.
[7] В.И. Альшиц, В.Н. Любимов. Кристаллография **33**, 279 (1988).
[8] В.И. Альшиц, В.Н. Любимов. ФТТ **45**, 222 (2003).
[9] В.И.Альшиц, В.Н. Любимов. ФТТ **45**, 1017 (2003).
[10] V.I. Alshits, M. Deschamps, G.A. Maugin. Wave Motion **37**, 273 (2003).
[11] В.И. Альшиц, В.Н. Любимов. ФТТ **45**, 832 (2003).

[12] V.I. Alshits, M. Deschamps, V.N. Lyubimov. J. Acoust. Soc. Am. **118**, 2850 (2005).
[13] R.D. Mindlin. In: Structural mechanics. Pergamon, N.Y. (1960). P. 199.
[14] A. Freedman. J. Sound Vib. **137**, 209 (1990).
[15] Q. Zhu, W.G. Mayer. J. Acoust. Soc. Am. **93**, 1983 (1993).
[16] A. Freedman. J. Acoust. Soc. Am. **98**, 2363 (1995).
[17] Л.Д. Ландау, Е.М. Лифшиц. Электродинамика сплошных сред. Наука, М. (1992). [L.D. Landau, E.M. Lifshits. Electrodynamics of continuous media. Pergamon, N.Y. (1984)].
[18] G.A. Maugin. Continuum mechanics of electromagnetic solids. North-Holland, Amsterdam (1988).
[19] Г.П. Мотулевич. УФН **97**, 211 (1969).
[20] Ю.И. Сиротин, М.П. Шаскольская. Основы кристаллофизики. Наука, М. (1975). [Yu.I. Sirotin, M.P. Shaskolskaya. Fundamentals of crystal physics. Mir, M. (1982)].
[21] И.А. Викторов. Физические основы применения ультразвуковых волн Рэлея и Лэмба в технике. Наука, М. (1966). [I.A. Viktorov. Rayleigh and Lamb waves: Physical Theory and Applications. Plenum Press, N.Y. (1967)].
[22] В.И. Альшиц, В. Герулски, В.Н. Любимов, А. Радович. Кристаллография **42**, 26 (1997).